

# Texture Analysis of Liver Tumor from Abdominal Computed Tomography in Computer Aided Diagnostic System

Gunasundari S<sup>1</sup>, Janakiraman S<sup>2</sup>

<sup>1</sup>Research Scholar, Pondicherry University, & Asst Prof, Velammal Engineering College

<sup>2</sup>Asst Prof, Pondicherry University

[gunapondyuniv@gmail.com](mailto:gunapondyuniv@gmail.com) , [jana3376@yahoo.co.in](mailto:jana3376@yahoo.co.in)

## Abstract

This paper proposes an automatic computer aided diagnostic system (CAD) for detection of liver diseases like hepatoma and hemangioma from Abdominal Computed tomography (CT) images. Liver and Lesion is segmented using gray level methods and clustering. Histogram analyzer is used to fix the threshold and morphological operation is used for post processing. Rules are applied to remove the obstacles. Fuzzy c-mean (FCM) clustering is used to extract the lesion from the segmented liver. First order statistical features, co-occurrence matrix based texture features, auto covariance features and Zernike moments are extracted from the segmented lesion. The sequential backward selection is applied to get the reduced feature set. The textual information obtained after feature reduction is used to train various neural networks such as a Probabilistic Neural Network (PNN) and Cascade feed forward BPN (CFBPN). The outcome obtained from neural networks is analyzed.

**Keywords** - FCM, Probabilistic Neural Network, Covariance Features, Co-occurrence matrix, Sequential Backward Selection, Zernike Moments, Liver

## 1. Introduction

Liver cancer is one of the leading causes of fatality in many developing countries. The most helpful way to decrease deaths due to liver cancer is to treat the disease in the early stages. The most frequent medical imaging studies for early recognition and analysis of liver cancers include ultrasonography (US), computed tomography, magnetic resonance imaging (MRI). CT is often the favored method for diagnosing many different cancers, since the image permits a physician to verify the presence of a tumor and to calculate its size and precise location. CAD systems have been developed to help doctors to identify

tumor precisely. The objective of the development of these systems is to help radiologists in interpreting radiographic images. Sometimes, cell development procedure goes wrong and can form a mass of tissue called a tumor. Tumors can be benign or malignant. Benign tumors are not cancer cells and do not extend to tissues around them. Cancer cells can attack and damage nearby tissues and organs. Hemangioma is a benign tumor consisting of masses of twisted, congested blood vessels. Malignant tumors are cancer. The Liver CAD system can be separated into four parts. The first part is the segmentation of the liver. The second part is the extraction of the lesion. The third part is the identification of features and the last one is the recognition or classification of the lesion. Many papers did not tackle the first and second part, assuming that the liver ROI (Region of Interest) has already been extracted. The lesion is to be separated from the liver to examine in detail for diagnosis. This paper is organized as follows. Section II presents the review of past work; Section III describes the proposed method for the classification of liver diseases from abdominal CT. Section IV discusses implementation and results. Finally, a brief conclusion and future work are included in Section V.

## 2. Past Work

Many liver texture analysis techniques have been proposed in the past for CT imaging modalities to take out useful features for reliable liver tissue classification. Support Vector Machine (SVM) is considered by some authors to differentiate liver diseases using features derived from abdominal CT. Huang et al (2006) selected the suspicious tumor region manually. The auto covariance texture features of sub image are extracted and SVM is used to build the liver disease identification system for testing the hepatic tumors as benign or malignant. The result shows that a total accuracy rate of 81.7% is obtained. Lee et al

(2007 a) implemented Kernel-based Classifier for classification of cyst, hepatoma and cavernous hemangioma. The multiclass SVM is used to identify the liver disease. Lee et al (2007 b) also proposed a multi class SVM classifier based on statistical learning theory for automatic classification in liver disease. Sobia (2008) obtained ROI by segmenting the liver from CT images using snake algorithm. The features are extracted using Spatial Gray Level Dependence Matrix (SGLDM). In order to classify liver diseases, the multiclass SVM is used. Wang et al (2009) used experienced radiologists to identify ROI with CT liver images. Texture features based on First Order Statistics (FOS), SGLDM, Gray Level run length matrix (GLRLM) and Gray level difference matrix (GLDM) are extracted for each ROI. Multi class SVM is used to classify liver diseases into primary hepatic carcinoma, hemangioma, and normal liver. The outcome shows that a total accuracy rate of 97.78% is obtained with the multiclass SVM using the one-against-one (OAO) method.

Neural networks have been extensively used in pattern classification applications. Mir et al (1995) characterized CT liver images into normal, visible and invisible malignancy. The statistical features are used to classify liver images. The results show that, it detects early malignancy with a confidence level of above 99%. Chen et al (1998) developed a CT liver image diagnostic classification system, which consists of a detect-before-extract (DBE) system, which automatically finds the liver boundary and a neural network liver classifier for classification. The classification rate obtained is about 83%. Mala et al. (2005) developed an automatic liver segmentation and classification system. The orthogonal wavelet transform is used to compute horizontal, vertical and diagonal information. Statistical texture features are extracted and PNN is used for classification. The proposed system produces an accuracy rate of 95%. Mala et al (2006 a) also extended their work to classify benign and malignant tumor using biorthogonal wavelet transform with Linear Vector Quantization (LVQ) network. The LVQ neural network is trained using the second order statistical texture features. The study and development of PNN, LVQ Neural Network and Back Propagation Network (BPN) for classification of fatty and cirrhosis liver diseases is reported in Mala et al (2010).

Kumar et al (2012) proposed automatic tumor segmentation, texture feature extraction, and characterization into malignant and benign tumors. An ROI is cropped from the automatically segmented tumor by confidence connected region growing and alternative FCM. Contourlet coefficients are obtained by decomposing the segmented ROI using a multi resolution and multidirectional Contourlet transform. Results indicate that the Contourlet coefficient texture is effective for classifying malignant and benign liver tumors. Kumar et al (2010, 2011, and 2012) reveals that transforms achieve better than wavelet transform for categorization. Using Curvelet and Contourlet transform he obtained the accuracy rate of about 94.3%. Mala et al (2010) and Gunasundari et al (2012) concluded that the performance of PNN is good when it is compared with other neural networks. They have obtained the accuracy of about 96%.

Glestos et al. (2001) developed a classifier consisting of three sequentially placed neural networks for four classes of hepatic tissues. Eight co-occurrence texture features are calculated for six different values of the pixel spacing. A total classification rate of 98% has been achieved. Mougiakakou et al. (2007) developed a CAD system architecture, which is able to accurately classify hepatic as normal liver, hepatic cyst, hemangioma, and HCC. For each CT liver ROI, five types of texture feature sets, based on FOS, SGLDM, GLDS, Laws Texture Energy Measure (TEM), and Fractal Dimension Measurement (FDM) are extracted. GA-based feature selection method is applied for feature selection. Appropriate voting schemes are used in the final decision of each classifier. Bharathi et al (2008) used orthogonal moments to classify the liver diseases from abdominal CT. The results show that the orthogonal moments like Zernike moments and Legendre moments features are successful texture descriptors

### 3. Proposed Method

In this paper, we describe a CAD system by means of Image processing techniques. CAD system is used to segment the liver in CT images using adaptive threshold and morphological opening and closing. Based on medical knowledge obstacles are detached automatically. The lesion is extracted using FCM. The textural features extracted from the

lesion are given as input to classifier to identify the disease. Overall system structure is shown in Fig. 1.

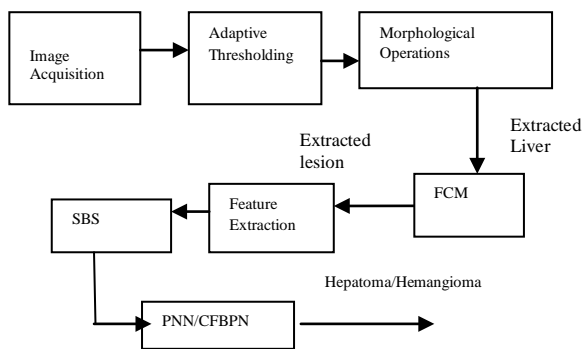


Figure 1: System Structure

### 3.1 Image Acquisition

The CT abdominal image is downloaded from the website ctisus.org, which is in JPEG format. CT is used and maintained by The Advanced Medical Imaging Laboratory (AMIL). AMIL is a multidisciplinary team dedicated to research, education, and the advancement of patient care using medical imaging with a focus on spiral CT and 3D imaging. The AMIL is part of the Department of Radiology at the Johns Hopkins Medical Institutions in Baltimore, Maryland. Images are done on a Siemens Sensation 64 MDCT (Multi Detector Computed Tomography).

### 3.2 Segmentation of Liver

In Liver Segmentation, Anatomic knowledge is used to locate the liver region. Normally the liver is located on the upper side of the image and takes up the major area in a CT image. Although the liver retains the constant intensity throughout, a fixed threshold is not possible since the intensity differs according to the patient slice and CT machine. The window size is fixed from a CT image. The histogram is drawn and analyzed for an area inside the window. The highest peak in the histogram represents the middle intensity of the liver region and certain intensities which are having high density are considered to fix the threshold. The pixels in the determined range of intensity are extracted. Morphological opening followed by closing is applied with the flat structuring element to smooth contours. Opening operation breaks narrow isthmuses, gets rid of sharp peaks whereas, closing operation fuses thin breaks, and eliminates little holes. Based on firm

conditions other regions located nearby in the liver can be detached. The first condition is the position of the object. The liver is located in a constant area in the upper left side of the image. The second condition is the area. The area of the liver is large when it is compared with the obstacles. The morphological operations are again applied after removing the obstacles. The image obtained after applying disk-structuring element is converted to binary image, complemented, and multiplied with the original image to get the segmented liver.

### 3.3 FCM for Lesion Extraction

There are many kinds of liver diseases like hepatoma, hemangioma, cysts, cholangiocarcinoma etc. It is not simple to discriminate between these diseases. To distinguish it, the lesion must be extracted. The extraction of lesion is also not simple. The threshold cannot be predetermined since the intensity of the lesion varies and it depends on CT machine. A technique independent of a varying intensity must be applied. This paper utilizes the version of the k-Means clustering and fuzzy logic. Fuzzy c-Means clustering is used to segment the lesion. The pixels of the input image are divided into 3 clusters. The first cluster includes pixels in the background. The second cluster includes pixels in the liver other than lesion and the third cluster includes pixels in the lesion. The post processing is done to remove some obstacles. Morphological closing followed by opening is applied again to the flat structuring element.

### 3.4 Feature Extraction

#### 3.4.1 Auto Covariance Features

Auto-correlation coefficients reflect the inter-pixel correlation within an image. It is a Mean removed version also called Modified Auto Covariance features. Let the given image has size  $M \times N$ . The modified auto-covariance coefficients are given by "Eq. (1)" and "Eq. (2)" [Huang et al 2006]

$$\gamma(\Delta m, \Delta n) = 1 - A(\Delta m, \Delta n)/A(0,0). \quad (1)$$

Where

$$A(\Delta m, \Delta n) = \frac{1}{(M - \Delta m)(N - \Delta n)} \times \left| \sum_{x=0}^{M-1-\Delta m} \sum_{y=0}^{N-1-\Delta n} (f(x, y) - mn)(f(x + \Delta m, y + \Delta n) - mn) \right| \quad (2)$$

Where  $\Delta m, \Delta n, a, b$  are positive constants

### 3.4.2 First order and Second Order statistical Features

FOS estimate properties of individual pixel values, disregard the spatial interaction between image pixels, FOS includes the features like mean, standard deviation, variance, kurtosis and skewness whereas second order statistics estimate properties of two or more pixel values occurring at specific locations relative to each other. Haralick et al. (1973) suggested the use of spatial gray level dependence matrices, which is based on the joint probability distributions of pairs of pixels. He described 14 statistics that can be calculated from the co-occurrence matrix.

### 3.4.3 Zernike Moments

Zernike moments are very dependent on the scaling and translation of the object, their magnitude is independent of its rotation angle. The Zernike polynomials are orthogonal thus; Zernike moments can be extracted from a segmented liver regardless of the shape. The computation of Zernike moments from an input image includes the computation of radial polynomials, the computation of Zernike basis functions and final one is the computation of Zernike moments by projecting the image onto the Zernike basis functions [Tahmasbi 2011]. The real-valued 1-D radial polynomial  $R_{n,m}$  is given by “Eq. (3)”

$$R_{n,m} = \sum_{s=0}^{(n-m)/2} (-1)^s \frac{(n-s)!}{(s \times ((n+m)/2 - s) \times ((n-m)/2 - s)!} \times \rho^{n-2s} \quad (3)$$

Where  $n$  is a non-negative integer representing the order of the radial polynomial,  $m$  is a positive or negative integer representing the repetition of the azimuthal angle.  $r$  is the length of vector from the origin to  $(x, y)$

Complex valued 2-D Zernike basis functions, which are defined within a unit circle, are formed by “Eq. (4)”

$$V_{n,m}(\rho, \theta) = R_{n,m}(\rho) e^{im\theta}, \quad |\rho| \leq 1 \quad (4)$$

The discrete form of the Zernike moments for an image with the size  $N \times N$  is expressed as follows in “Eq. (5)” to “Eq. (7)”

$$Z_{n,m} = \frac{(n+1)}{\lambda_n} \times \sum_{c=0}^{N-1} \sum_{r=0}^{N-1} f(c, r) R_{n,m}(\rho_{cr}) e^{-jm\theta_{cr}} \quad (5)$$

Where

$$0 \leq \rho_{cr} \leq 1$$

$\lambda_n$  is a normalization factor

Transformed distance and phase is given by

$$\rho_{cr} = \frac{\sqrt{(2c - N + 1)^2 + (2r - N + 1)^2}}{N} \quad (6)$$

$$\theta_{cr} = \tan^{-1} \left( \frac{N - 1 - 2r}{2c - N + 1} \right) \quad (7)$$

### 3.5 Feature Reduction

Feature selection selects the subset of features to decrease the feature space, which get better the prediction accuracy and reduce the computation time. This is achieved by removing inappropriate, unneeded, and noisy features. It does the Dimensionality reduction. Filter methods assess each feature independently with respect to the class labels in the training set, and decide a ranking of all features, from which the top ranked features are selected. Wrapper methods use classic Artificial Intelligence search methods to look for the best subset of features, repetitively assessing dissimilar feature subsets via cross validation with a particular induction algorithm. We have used wrapper-based method for feature selection. Wrappers usually achieve better detection rates than filters since they are adjusted to the precise interactions between the classifier and the data set and it has capability to generalize since they typically use cross-validation procedures of predictive accuracy

#### 3.5.1 Sequential forward selection (SFS) and Sequential backward selection (SBS)

SFS selects a subset of features from the feature vector that best predict the disease by successively selecting features until there is no progress in prediction. Objective function defines the criterion that is used to select features and to determine when to stop. The output is a logical vector indicating which features are finally chosen. Starting from an empty feature set, SFS creates candidate feature subsets by sequentially adding each of the features not yet selected. For each candidate feature subset, it performs 10-fold cross-validation by repeatedly calling criterion with different training feature vector and test data. It computes the misclassification rate. It



sums the values returned by criterion function and divides that sum by the total number of test observations. It then uses that mean value to evaluate each candidate feature subset. It calculates the mean-squared error. After calculating the mean criterion values for each candidate feature subset, it chooses the candidate feature subsets that lessen the mean criterion value. This process carries on until adding more features does not diminish the criterion. SBS specifies an initial candidate set including all features and an algorithm that remove features in sequence until the criterion decrease.

### 3.6 Classification

Neural networks are ideal in recognizing diseases using scans since there is no need to provide a exact algorithm on how to recognize the disease. The segmented lesion is given as input to feature extraction module. The reduced statistical features are given as input to CFBNP and PPN to distinguish the diseases.

**Cascade Feed Forward Back propagation Neural Network (CFBPN):** BPN provides better answer to pattern classification problem. BPN is known as learning in feed-forward networks in which pairs of input and output values are fed into the network for many cycles, so that the network is trained the relationship between the input and output. CFBPN is like BPN but it comprises a weight connection from the input to each layer and from each layer to the successive layers.

**Probabilistic Neural Network (PNN):** PNN is a feed forward neural network constructed with three layers. They are derived from Bayes Decision Networks. They train speedily since the training is done in one pass of each training vector, rather than numerous. In a PNN, the operations are organized into a multilayered feed forward network with four layers such as Input layer, Hidden layer Pattern layer/Summation layer and Output layer. Probabilistic neural networks calculate approximately the probability density function for each class based on the training samples. In categorical variables, N-1 neurons are used when there are N numbers of group. It standardizes the range of the values by deducting the median and dividing by the interquartile range. Then the input neurons

feed the values to each of the neurons in the hidden layer. Hidden layer contains one neuron for each case in the training data set. It stores the values of the predictor variables in the case along with the target value. A hidden neuron calculates the Euclidean distance of the test case from the neuron's center point and then applies the RBF kernel function with the sigma values. In Summation layer the pattern neurons add the values for the class they represent. The output layer compares the weighted votes for each target category accumulated in the pattern layer and uses the largest vote to predict the target category. PNNs are much quicker than multilayer perceptron networks and it can be more accurate than multilayer perceptron networks.

### 4. Implementation and Results

The abdominal CT images are downloaded from the website ctisus.org and stored as a JPEG file. The total number of different image slice considered for evaluation is 48. It includes 36 hepatoma and 12 hemangioma images. Since the liver is located in the left side of the CT image, the window slice including liver and other obstacles in the window is selected. Then the histogram is drawn to this window and analyzed. The intensity points with the maximum count are identified to fix the threshold. The pixels in the determined range of intensity are extracted (Fig. 2). Morphological operations are applied and obstacles are removed from the rules. The lesion is extracted using FCM.

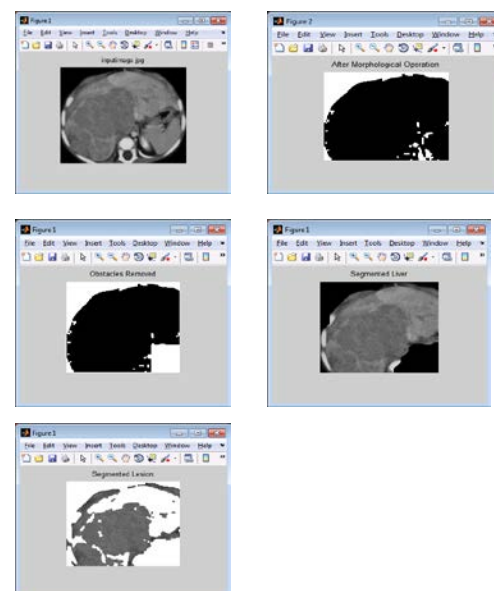

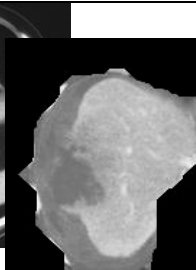


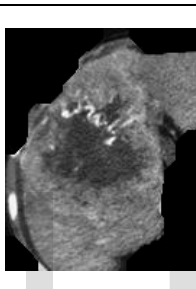



Figure 2: Output of Segmentation of Liver

The segmentation output for some images is shown in Table 1. The auto covariance, FOS, SGLDM, and Zernike moments are extracted from the lesion.

**Table 1: Segmentation Output for some Images**

Input Image	Segmented Liver	Segmented Lesion
		
		

While calculating auto covariance features the positional difference varies from 1 to 12. The number of features extracted varies based on positional difference values. The possible feature set extracted is 2, 5, 9, 14, 27, 44, 65, and 90 (Table 2).

The derived textural features are given as input to classifiers individually for classification of disease and for analyzing the performance. The 33 images are considered for training and 15 images are considered for testing. Performance of different networks for various features is evaluated by calculating Accuracy, Sensitivity, Specificity, Positive predictive value (PPV) and Negative predictive value (NPV).

Parameters	Formula
Accuracy	$(TP+TN) / (TP+TN+FP+FN)$
Sensitivity	$TP / (TP+FN)$
Specificity	$TN / (TN+FP)$
PPV	$TP / (TP+FP)$
NPV	$TN / (TN+FN)$

True Positive (TP): lesions called hepatoma and prove to be hepatoma. False Positive (FP):

lesions called hepatoma that proves to be a hemangioma False Negative. (FN): lesions that are called hemangioma and prove to be hepatoma. True Negative (TN): lesions that is called hemangioma and proves to be hemangioma. The training sets produced the accuracy of 100% of all textural features whereas testing set produces a different performance and hence it is analyzed. The Performance of PPN and CFBN for Covariance features with different positional differences and the time taken to extract features for all images are shown in Table 2. The features are also given to the feature selection module to fetch the best feature set. Both SFS and SBS are implemented and analyzed. SBS performs well to select the best feature set to have a good accuracy rate of about 98%. Covariance features space is also reduced using SBS and result is shown in Table 3. The time taken to extract features for classification after feature reduction using SBS is minimized

In FOS, the mean, standard deviation, variance, kurtosis and skewness are derived from the lesion. SGLDM is constructed for the given lesion by varying the distance (d=2, 4, 6) and degree (0 and 45). For all co-occurrence matrices, features like energy, Contrast, Correlation, Sum of Variances, Inverse Difference Moment, Sum Average, Sum Variance, Sum Entropy, Entropy, Difference Variance, Difference Entropy Information Measures Correlation1 and Information Measures Correlation2 are extracted. Based on the performance of the classification the degree 0 and distance 4 is selected. The SGLDM features are calculated with d=4, and degree =0 and it is analyzed with different combination of features after feature reduction using SBS (Table 4). During classification, the accuracy rate is about 98% for PNN whereas in CFBN it is 90%. FOS with SGLDM features after feature reduction shows the improvement in accuracy rate of 2%.

Zernike moments are derived from the segmented liver using radial polynomial by varying m and n. For m=2 and n=4, the system performs well to produce the accuracy of 94%. The performance review of various textural features using classifier is shown in Table 5. The result shows that the sensitivity of all methods is 100%. From Table 3-5, it is evident that performance of classifier for SGLDM features is superior to other features.

**Table 2: Auto Covariance Features for different ( $\Delta m, \Delta n$ )**

Max value of ( $\Delta m + \Delta n$ ), Possible values of ( $\Delta m, \Delta n$ )	No of Features	Accuracy with PNN (%)	Accuracy with CFB PN	Time in (Seconds) Feature Extraction
1 (0,1)(1,0)	2	75	75	2.1
2 (0,1),(1,0),(1,1),(2,0),(0,2)	5	75	75	2.3
3 (0,1),(1,0),(1,1),(2,0),(0,2), (1,2),(2,1),(3,0),(0,3)	9	79	75	2.7
$\Delta m + \Delta n = 4$ (0,1),(1,0),(1,1),(2,0),(0,2), (1,2),(2,1),(3,0),(0,3),(0,4), (4,0),(1,3),(3,1),(2,2)	14	83	75	3.4
$\Delta m + \Delta n = 6$ (0,1),(1,0),(1,1),(2,0),(0,2),(1,2),(2,1), (3,0),(0,3),(0,4),(4,0),(1,3),(3,1),(2,2), (0,5),(5,0),(1,4),(4,1),(2,3),(3,2), (0,6),(6,0),(1,5),(5,1),(2,4), (4,2),(3,3)	27	90	75	3.9
$\Delta m + \Delta n = 8$ (0,1),(1,0),(1,1),(2,0),(0,2),(1,2),(2,1), (3,0),(0,3),(0,4),(4,0),(1,3),(3,1),(2,2), (0,5),(5,0),(1,4),(4,1),(2,3),(3,2), (0,6),(6,0),(1,5),(5,1),(2,4), (4,2),(3,3), (0,7),(7,0),(6,1), (1,6),(2,5),(5,2),(3,4),(4,3),(0,8),(8,0), (1,7),(7,1),(2,6),(6,2),(3,5),(5,3),(4,4)	44	94	92	5.5
$\Delta m + \Delta n = 10$ (0,1),(1,0),(1,1),(2,0),(0,2),(1,2),(2,1), (3,0),(0,3),(0,4),(4,0),(1,3),(3,1),(2,2), (0,5),(5,0),(1,4),(4,1), (2,3),(3,2),(0,6),(6,0),(1,5),(5,1),(2,4), (4,2),(3,3), (0,7),(7,0),(6,1),(1,6),(2,5),(5,2),(3,4), (4,3),(0,8),(8,0),(1,7),(7,1),(2,6),(6,2), (3,5),(5,3),(4,4),(0,9),(9,0),(8,1), (1,8),(2,7),(7,2),(3,6),(6,3),(5,4),(4,5), (0,10),(10,0),(1,9),(9,1),(2,8),(8,2), (3,7),(7,3),(4,6),(6,4),(5,5)	65	96	92	7.3
$\Delta m + \Delta n = 12$ (0,1),(1,0),(1,1),(2,0),(0,2),(1,2),(2,1), (3,0),(0,3),(0,4),(4,0),(1,3),(3,1),(2,2), (0,5),(5,0),(1,4),(4,1), (2,3),(3,2),(0,6),(6,0),(1,5),(5,1),(2,4), (4,2),(3,3), (0,7),(7,0),(6,1),(1,6),(2,5),(5,2),(3,4), (4,3),(0,8),(8,0),(1,7),(7,1),(2,6),(6,2), (3,5),(5,3),(4,4),(0,9),(9,0),(8,1), (1,8),(2,7),(7,2),(3,6),(6,3),(5,4),(4,5), (0,10),(10,0),(1,9),(9,1),(2,8),(8,2), (3,7),(7,3),(4,6),(6,4),(5,5),(0,11),(11,0), (10,1),(1,10),(2,9),(9,2),(3,8),(8,3), (4,7),(7,4),(5,6),(6,5),(0,12),(12,0), (11,1),(1,11),(2,10),(10,2),(3,9),(9,3), (4,8),(8,4),(5,7),(7,5),(6,6)	90	96	92	8.1

**Table 3: Covariance Features (Before and After Feature Reduction)**

No of Features, Selected Features	Accuracy	Sensitivity	Specificity	PPV	NPV
90 (1-90)	98	100	92	97	100
45 (15-17,22-23,29-30,53-90)	98	100	92	97	100
30 (6,10,11,16,22,66-90)	96	100	83	95	100
15 (16,22,78-90)	96	100	83	95	100

**Table 4: SGLDM Features (Before and After Feature Reduction)**

No of Features, Features Selected	Accuracy	Sensitivity	Specificity	PPV	NPV
13 features (1-13)	96	100	83	95	100
9 features (1-6,8-11)	<b>98</b>	100	92	97	100
7 features (1-3,5,6,8,9)	96	100	83	95	100
5 features (1,2,3,5,6)	96	100	83	95	100

**Table 5 Performance Summary of textural features in PNN**

Features	Accuracy	Sensitivity	Specificity	PPV	NPV	Time in (Seconds) Feature Extraction
FOS	92	100	66	90	100	0.002
GLCM (d=4, degree 0) 9 Features	<b>98</b>	100	92	97	100	<b>0.3</b>
Auto Covariance (45 Features)	98	100	92	97	100	5.4
Zernike Moments	94	100	75	92	100	0.1
FOS+GLCM (18 Features)	94	100	75	92	100	0.3

## 5. Conclusion and Future Work

The proposed CAD system is used to segment the liver using adaptive threshold followed by morphological operations. The lesion is extracted using FCM. The segmentation algorithm proves to be simple, but effective. The statistical, Zernike moment and auto covariance features are extracted from the segmented lesion. The best features are selected using SBS. The best features are given as input to a classifier like CFBN and PNN to classify hepatoma and hemangioma. In comparisons, SGLDM and auto covariance features yields had better result in PNN with the high accuracy of 98%. Gray scale co-occurrence matrix performed well in PNN with the accuracy rate 98% with the reduced feature set. The performance of PNN is good when it is compared with other classifiers for this feature set. In future, it will be tested on a large number of images and different type of diseases.

## Acknowledgement

Author would like to thank Elliot K. Fishman, M.D., Professor, Radiology and Oncology Director, Diagnostic Imaging and Body CT, Johns Hopkins Medical Institutions in Baltimore, Maryland for providing us abdominal CT image through CT is us website to do our research work.

## References

1. Bharathi VS, Ganesan L (2008) Orthogonal moments based texture analysis of CT liver images. *Pattern Recognition Letters* 29:1868–1872
2. Chen EL, Chung PC, Chen CL, Tsai HM, Chang CI (1998) An Automatic Diagnostic System for CT Liver Image Classification. *IEEE Transactions on Biomedical Engineering* 45:6:783-794
3. Glestos M, Mougiakakou SG, Matsopoulos GK., Nikita KS, Nikita, AS, Kelekis D (2001) Classification of hepatic lesions from CT images using texture features and neural networks. In: *Proc. Of 23rd Annual EMBS International Conference of IEEE on Engineering in Medicine and Biology Society* 3: 2748–2752
4. Gunasundari S, Suganya Ananthi M (2012) Comparison and Evaluation of Methods for Liver Tumor Classification from CT Datasets. *International Journal of Computer Applications* 39:18:46 -51
5. Haralick RM, Shanmugam K, Dinstein I (1973) Texture features for image classification. *IEEE Transaction on System, Man and Cybernetics SMC-3* (6) : 610-621
6. Huang, YL, Chen JH, Shen WC (2006) Diagnosis of Hepatic Tumors with Texture Analysis in Non enhanced Computed Tomography Images. *Acad Radiol* 2006 13:713–720
7. Kumar SS, Moni RS (2010 a) Diagnosis of Liver Tumor from CT Images using Curvelet Transform. *International Journal on Computer Science and Engineering* 2:4: 1173-1178
8. Kumar SS, Moni RS (2010 b) Diagnosis of Liver Tumor from CT Images using Curvelet Transform. *International Journal of Computer Application Special Issue on CASCT* 1:1-6
9. Kumar SS, Moni RS, Rajeesh J (2011) Contourlet Transform Based Computer-Aided Diagnosis System for Liver Tumors on Computed Tomography Images. In: *Proc. of International Conference of IEEE on Signal Processing, Communication, Computing and Networking Technologies* 217 - 222
10. Kumar SS, Moni RS, Rajeesh J (2012) Liver tumor diagnosis by gray level and contourlet coefficients texture analysis. *International Conference on Computing, Electronics and Electrical Technologies* 557 – 562
11. Lee CC, Chiang YC, Tsai CL, Chen SH (2007 a) Distinction of Liver Disease from CT images using Kernel-based Classifiers. *ICMED*, 1:2:113-120
12. Lee CC, Chen SH, Chiang YC (2007 b) Classification of Liver Disease from CT Images Using a Support Vector Machine. *Journal of Advanced Computational Intelligence and Intelligent Informatics* 11:4: 396-402
13. Mala K, Sadasivam V (2005) Automatic segmentation and



- classification of diffused liver diseases using wavelet based texture analysis and Neural Network. In Proc of International Conference of IEEE on INDICON 216-219
14. Mala K, Sadasivam V (2006 a) Wavelet based texture analysis of Liver tumor from Computed Tomography images for characterization using Linear Vector Quantization Neural Network. In: Proc. Of International conference of IEEE on Advanced Computing and Communication 267 - 270
15. Mala K , Sadasivam S (2010) Classification of Fatty and Cirrhosis Liver Using Wavelet-Based Statistical Texture Features and Neural Network Classifier. International Journal of Software Informatics 4:2:151-163
16. Mir AH, Hanmandlu M, Tandon SN (1995) Texture analysis of CT images. IEEE Engineering in Medicine and Biology 14: 6:781-786
17. Mougialakou SG, Valavanis I, Nikita A, Nikita KS (2007) Differential diagnosis of CT focal liver lesions using texture features, feature selection and ensemble driven classifiers. Artificial Intelligence in Medicine 41:25—37
18. Srinivasan GN, and Shobha G. (2008) Statistical Texture Analysis. In: Proc. of World Academy of Science, Engineering And Technology 36: 1264-1269
19. Sumit G, Gyandera Kumar G Cascade and Feedforward Backpropagation Artificial Neural Network Models For Prediction Of Sensory Quality of Instant Coffee Flavoured Sterilized Drink. Canadian Journal on Artificial Intelligence, Machine Learning and Pattern Recognition Vol. 2, No. 6 August 2011
20. Tahmasbi A, Saki F, Shokouhi SB (2011) Classification of benign and malignant masses based on Zernike moments, Computers in Biology and Medicine 41 (2011) 726–735
21. Wang L, Zhang Z , Liu J, Jiang B, Duan X, Xie Q, Hu D, Li Z (2009) Classification of Hepatic Tissues from CT Images Based on Texture Features and Multiclass Support Vector Machines. In: Proc of International Symposium on Neural Networks: Advances in Neural Networks 374-381